S- and X-Band Feed System

P. D. Potter
Communications Elements Research Section

In support of the Mariner 1973 X-band experiment, it is necessary to provide the DSS 14 64-meter-diameter antenna with a dual-frequency microwave feed system. To fulfill this requirement, a particularly attractive approach, the reflex feed system, has been implemented. Completion of the reflex feed installation into the DSS 14 antenna was accomplished on January 24, 1973. The performance of this system was evaluated during the period of January 25, 1973, through January 30, 1973. This evaluation established the reflex feed system performance as completely acceptable to the Mariner 1973 X-band experiment. In two cases, S-band antenna gain and S-band system noise temperature, the reflex feed system performance is actually superior to the standard S-band feed system. In this reporting the feed system design is briefly reviewed, including a new dichroic reflector developed at JPL, and the performance measurement data are presented.

I. Dichroic Reflector Design

A cross-sectional view of the reflex feed system geometry is shown to scale in Fig. 1. For correct operation, the planar dichroic reflector must appear to the 2.1- and 2.3-GHz S-band signals as though it were an essentially perfectly relative, flat surface. To the 8.4-GHz X-band signal, the dichroic reflector must appear essentially transparent and loss-free. Moreover, these performance characteristics must be reliably maintained under all of the normal environmental conditions of gravity, sun, rain, wind, dirt, high-power transmission, etc.

Calculations of the S-band high-power transmission-induced heat dissipation in the dichroic reflector were reported in Ref. 1. The solar flux provides an additional heating effect. A detailed thermal analysis, performed in mid-1972 by the Temperature Control and Radiation Section, showed a serious thermal problem to exist if a thin dichroic reflector was utilized. The calculated S-band performance effects of thermally induced physical distortions of the dichroic plate were reported in Ref. 2. These calculations showed that the dichroic reflector has to maintain an extremely flat surface (to within the order of a few millimeters) to avoid serious pattern distortion and resultant increase in forward spillover-induced system noise temperature.

The original dichroic reflector design concept was derived from a thin, narrow-band system developed at Ohio

State University. The Ohio State design was modified by Woo and Ludwig (Refs. 3 and 4) for improved polarization characteristics. Subsequently it was discovered in noise-temperature measurements by D. Nixon of the Communications Elements Research Section that this dichroic reflector design possessed severe X-band dissipative loss because of its narrow bandwidth of operation. The design was broadband by Bathker, Nixon, and Kurtz[1] and the plate thickness increased to 3 millimeters, both without performance degradation.

Because of the physical stability problem of the dichroic reflector described above and its susceptibility to degradation by foreign material (paint, dirt, etc.), an alternate approach was investigated. This alternate approach consists of a thick flat plate perforated with circular holes. Such a device may be analyzed from a phased-array standpoint (Ref. 5), or by more explicit boundary-value problem techniques (Ref. 6). A sample dichroic plate of this type (Fig. 2) was constructed and tested. Using simple but powerful conservation-of-energy techniques, Hannan (Ref. 5) derives the conditions for scan-independent matched phased arrays. His results are directly applicable to dichroic plates of the type shown in Fig. 2 and predict that such a plate is essentially guaranteed to work reasonably well.

The design procedure for the sample plate (Fig. 2) was extremely simple. The hole diameter was selected to be somewhat larger than the dominant circular TE_{11} mode waveguide cutoff size (a ratio of guide to free space wavelength of 2 was selected), as a compromise between tolerance sensitivity and excess element spacing. To minimize the latter, hexagonal packing was utilized.[2] The hole separation was minimized to the extent compatible with conventional machine shop practice. The plate was made 3.81 cm thick (1.5 in.), a readily available size of tooling plate, and approximately 35 cm square.

Using the standard formulas for smooth-wall waveguide losses, the X-band dissipative loss of the dichroic plate was calculated as 0.8 K, vs a measured value of 1.2 K. This discrepancy has not been satisfactorily explained. Of more significance to the Mariner 1973 Project is the increased loss at S-band relative to a nonperforated plate. To evaluate this effect, a scale model was made (Fig. 3) so that S-band performance tests could be made at X-band. The increased surface resistivity was measured as a ratio of 2.6, relative to a nonperforated plate, by a cavity-Q technique (Ref. 7). For standard aluminum alloy a resulting noise contribution of 0.17 K is predicted. Because of the large plate thickness, there is essentially no S-band leakage (approximately −50 dB) through the plate. The effect of paint, dirt, water, etc., on the dichroic plate performance was experimentally determined; all effects proved negligible except for heavy water accumulation in the holes. This problem could occur in a heavy rainstorm at DSS 14. It is serious but can be overcome.

The prototype plate (Fig. 2) transparent frequency is 7.9 GHz; the final design (Fig. 4) installed at DSS 14 is a simple frequency scale of the prototype plate, by the ratio 7.9/8.4. Prior to installation on the DSS 14 antenna, this final plate was tested with the multiple-frequency X- and K-band (MXK) feedcone at the Goldstone Microwave Test Facility (MTF). An X-band degradation, relative to no dichroic plate, of approximately 5 K was expected from a measured −18 dB X-band reflection coefficient for the plate (see Fig. 1). This large (5 K) degradation results from the reflected lobe "seeing" the warm ground. With the X-band feedhorn directed toward zenith, and the cone on the ground at MTF, a value of 5.6 K was actually measured.

Three performance parameters of this dichroic reflector leave room for substantial improvement; all result from the fact that the tilted-plate E- and H-plane fully-transparent frequencies are slightly different. For circular polarization, the overall reflection coefficient is −18 dB, giving rise to a significant X-band noise temperature contribution as a function of antenna elevation angle. Secondly, a differential phase shift between the E- and H-planes gives rise to an X-band depolarization effect, resulting in an ellipticity of 1.8 dB. For a perfectly circularly polarized spacecraft signal, the resultant link loss is −0.04 dB and for a 3.0-dB spacecraft ellipticity the maximum link loss is −0.32 dB. A promising technique for simultaneously curing both of these deleterious dichroic plate effects is presently under investigation. The third and most serious problem is the effect of rain water accumulation. Techniques for surface modification to reduce water droplet formation are being investigated.

II. Measured Performance: Focus and Boresight Characteristics

During the period January 25–30, 1973, extensive tests were performed at DSS 14 on the reflex feed system to

[1]L. Kurtz, consultant to JPL Communications Elements Research Section.

[2]Suggested by R. Clauss of the JPL Communications Elements Research Section.

determine its performance parameters.[3] Selected analysis was done in preparation for these tests; possible problem areas in the system were differential focus and boresight characteristics between the two frequency bands. The mechanism for the possible focusing difficulty is discussed in Ref. 2. In preparation for the focus tests a nonlinear curve-fitting computer program was developed for real-time reduction of antenna gain vs focus position data. This program determines the focus maximum and the magnitude and phase of the sinusoidal component caused by subreflector mismatch. Fortunately, this effect proved to be negligible at both S- and X-bands for the reflex feed. The optimum focus positions were found to agree well with the prior nonreflex feed positions for S- and X-band.

It was expected that there would be differential boresights for the four different conditions of S- and X-band and reflex vs nonreflex operation. Therefore, an important first step in the DSS 14 tests was to determine the boresight positions of the antenna beam maxima. In preparation for these tests, the Ludwig Scattering Program (Ref. 8) was used to calculate the effects of longitudinal displacements, parallel to the S-band megawatt transmit (SMT) and MXK cone axes, of the ellipsoidal and planar reflectors. Such displacements are a practical field technique for adjusting the S-band reflex antenna beam position relative to the X-band beam position. These calculations were an extension of those previously performed (Ref. 9) during the feed system design. Longitudinal displacements of ± 12.7 cm (5.0 in.) of both the ellipsoid and planar reflector were investigated. Scattered patterns, referenced to the optically imaged phase center points of the displaced reflectors, were computed and found to have indiscernible degradations relative to the nominal reflex feed configuration (Fig. 1). Thus the technique of longitudinal reflector displacement was shown to be effective and practical for correction of reflex feed system differential boresight difficulties.

Preliminary boresight tests performed on the night of January 25 (Universal Time) indicated that a 2.54-cm (1.0-in.) outward displacement planar reflector would bring the S-band reflex antenna beam into good alignment with the X-band reflex beam. This correction was performed,[4] by shimming, on the following day and has become a permanent part of the installation. Subsequent tests quantitatively demonstrated that this technique produces a boresight shift which, in magnitude and direction, is exactly predicted by simple geometric considerations.

The fact that the reflex feed was designed for rapid, remote changeover to nonreflex operation allowed for rapid reliable measurement of differential boresight positions. In addition to the standard half-power boresight method, a new technique was tried in which the antenna pointing was stepped by known amounts relative to the ephemeris radio source position and radiometer response was recorded. A least-squares fit of these data to a Gaussian antenna beam was performed in quasi-real-time on the DSS 14 SDS930 computer. This technique proved to be somewhat tedious, but a high level of repeatability was achieved (always better than 0.001 deg, and typically 0.0005 deg).

The results of the boresight tests are shown in Fig. 5. This figure is a view of the true beam positions as seen by an observer facing the antenna aperture. The figure is in the Cartesian antenna coordinates of elevation and cross-elevation. The SMT feedcone nonreflex beam is, by definition, in the center of the coordinate system. Because the plane containing the two cone axes makes a 30-deg angle with the elevation plane, and because the reflex feed system is physically symmetrical with respect to the plane containing the two cone axes, the adjustment procedure described above moves the S-band reflex beam on a line making a 30-deg angle with respect to the vertical axis in Fig. 5. It can be seen that, within this constraint, the 2.54-cm adjustment performed was optimum in terms of minimizing the S- and X-band reflex beam position separation.

The lateral S-band reflex beam offset (perpendicular to the 30-deg line) is quantitatively explainable (in retrospect) in terms of an ellipsoid-induced beam symmetry effect peculiar to circular polarization. As explained in Ref. 9, the ellipsoid radiation may be analyzed in terms of cos $(m\phi)$ and sin $(m\phi)$ azimuthal variations, where ϕ is the azimuthal angle of the radiation. Figure 2 of Ref. 9 is reproduced here as Fig. 6 and shows qualitatively the field distribution corresponding to these azimuthal Fourier components. The $m = 1$ component is desired for high efficiency; the ellipsoid introduces significant $m = 0$ and $m = 2$ energy, however (see Fig. 3 of Ref. 9). As can be seen in Fig. 6, each of these components introduces an antisymmetrical (e.g., in the sense of a monopulse error channel) cross-polarized radiation component. This component combines with the desired symmetrical circular polarization component to produce a beam shift. The

[3]These tests, which were conducted under the direction of G. Levy, were performed by D. Bathker, A. Freiley, G. Levy, F. McCrea, D. Nixon, P. Potter, C. Stelzried, and H. Reilly, all of the Communications Elements Research Section.

[4]This adjustment was done under the direction of H. R. Hoggan, DSIF Engineering Section.

SMT cone is set up for right-hand circular polarization (RCP); although not tested, it is predicted that left-hand circular polarization (LCP) would display a boresight deviation (relative to the 30-deg line) of the same magnitude as RCP but of opposite direction.

The shift between the reflex and nonreflex X-band beams is primarily caused by the thick dichroic reflector —the so-called "dogleg" effect. The measured direction of the effect is almost exactly as expected, but the magnitude is about 30% too large, for unexplained reasons.

III. Measured Performance: Antenna Gain

The predicted S-band gain was given in Ref. 1. Those figures must be slightly modified, however, since they assumed use of the original thin dichroic reflector (both physical distortion and transmission losses were assumed). The gain differential between the two S-band systems was independently measured by two different teams: Bathker and Freiley and Nixon and Potter. The former utilized the radio source 3C123; the latter utilized the radio source 3C273. In reducing these data, antenna elevation angle variations were minimized by curve-fitting. The two measurement results and the upgraded prediction are as follows:

$$(G_{\mathrm{dB}_{\mathrm{reflex}}} - G_{\mathrm{dB}_{\mathrm{SMT}}})_{\substack{\text{calculated:}\\ 2.295\ \text{GHz}}} = -0.05 \pm 0.05\ \text{dB, p.e.} \quad (1)$$

$$(G_{\mathrm{dB}_{\mathrm{reflex}}} - G_{\mathrm{dB}_{\mathrm{SMT}}})_{\substack{\text{measured:}\\ \text{Bathker and}\\ \text{Freiley,}\\ 2.295\ \text{GHz}}} = -0.03 \pm 0.01\ \text{dB, p.e.} \quad (2)$$

$$(G_{\mathrm{dB}_{\mathrm{reflex}}} - G_{\mathrm{dB}_{\mathrm{SMT}}})_{\substack{\text{measured:}\\ \text{Nixon and Potter,}\\ 2.295\ \text{GHz}}} = -0.02 \pm 0.01\ \text{dB, p.e.} \quad (3)$$

In combining these data for a best estimate of antenna gain differential, it is assumed that (2) and (3) are *not* statistically independent, but the combination of (2) and (3) *is* independent of (1). The result is

$$(G_{\mathrm{dB}_{\mathrm{reflex}}} - G_{\mathrm{dB}_{\mathrm{SMT}}})_{\substack{\text{final,}\\ 4/4/73,\\ 2.295\ \text{GHz}}} = -0.03 \pm 0.01\ \text{dB, p.e.} \quad (4)$$

In (1) through (4), tracking on the X-band reflex beam peak is assumed.

The measurement of differential X-band reflex vs nonreflex antenna gain was seriously constrained by limited time. The result of the measurement is as follows:

$$(G_{\mathrm{dB}_{\mathrm{reflex}}} - G_{\mathrm{dB}_{\mathrm{MXK}}})_{\substack{\text{measured:}\\ \text{Bathker and}\\ \text{Freiley,}\\ \text{random}\\ \text{polarization,}\\ 8.415\ \text{GHz}}} = -0.06 \pm 0.05\ \text{dB, p.e.} \quad (5)$$

Fortunately, for this case, a rather accurate analytic prediction is possible. The three effects of the dichroic reflector are (1) reflective loss (−0.04 dB), (2) dissipative loss (−0.02 dB), and (3) depolarization loss (−0.04 dB for an RCP source). For a randomly polarized source such as that used in these gain tests (3C123), the last of these effects is not observed. The predicted gain differential is therefore in agreement with the measured value. The final result for RCP polarization is:

$$(G_{\mathrm{dB}_{\mathrm{reflex}}} - G_{\mathrm{dB}_{\mathrm{MXK}}})_{\substack{\text{final,}\\ 4/4/73,\\ \text{RCP polarization,}\\ 8.415\ \text{GHz}}} = -0.10 \pm 0.02\ \text{dB, p.e.} \quad (6)$$

IV. Measured Performance: System Noise Temperature

In the process of making the radio source noise temperature measurements necessary for the gain tests, a large volume of off-source system noise temperature data was collected. Figure 7 shows a cubic polynomial spline curve-fit to the measured S-band data. Figure 8 similarly shows the X-band data. The 1 sigma variation of the data relative to the simple curve-fit is better than 0.1 K in all cases. This is felt to be a result of excellent system stability, the excellent noise-adding radiometer (NAR) stability, and good weather conditions (clear, dry, cold).

The elevation angle is plotted in Figs. 7 and 8 on a special nonlinear scale such that the standard cosecant (elevation angle) flat-earth atmospheric effect will plot as a straight line. It is clear from these plots that antenna-spillover/quadripod scattering effects exist which make the measured curves highly nonlinear on this type of plot. The atmospheric loss contribution shown in Fig. 7 for S-band is well established (Ref. 10) and at that frequency can have only minor dependency on atmospheric water content. The superior noise temperature performance of the S-band reflex feed system relative to the standard SMT systems arises from at least two sources: lower forward spillover (Ref. 1) and the fact that, because of

the tricone system geometry, the SMT feed system points approximately 8 deg lower in elevation than the S-band reflex feed system.

In the X-band data, two atmospheric loss curves are shown. The lower (2.5 K at zenith) is predicted for dry, cold winter conditions[5] such as those prevailing during the tests. The upper curve (3.5 K at zenith) corresponds to very humid, hot weather or possibly cloud cover conditions.

V. Summary

For purposes of the Mariner 1973 X-band experiment, the recently installed and evaluated DSS 14 prototype reflex dichroic S/X feed system is considered entirely adequate. Prime S-band system gain and system noise temperatures are within 0.03 dB and 2.0 K of the original nonreflex performance (noise temperature improvement). The experimental X-band system is within 0.10 dB and 2.0 K of the original nonreflex performance (the X-band numbers are degradations). Coincidence of all four possible beams (two nonreflex and two reflex) has been established with negligible error and is adequate. It is expected that the MVM 73 Project will adopt tracking on the X-band reflex beam peak; the negligible loss to the S-band performance is included within the 0.03 dB S-band loss mentioned above.

Improved noise-adding radiometer performance during the extended test period together with a new presentation of system noise temperatures as functions of elevation angle with a reduced X-band estimate of atmospheric zenith loss contribution points out that spillover and quadripod scattering effects have always existed. These data will be considered in conjunction with another antenna noise performance improvement program.

Substantial improvements in the dichroic plate appear possible and will be considered.

[5]Extensive unpublished calculations of atmospheric noise contributions have been performed by T. Otoshi of the Communications Elements Research Section.

References

1. Potter, P. D., "S- and X-Band RF Feed System," in *The Deep Space Network Progress Report*, Technical Report 32-1526, Vol. IX, pp. 141–146, Jet Propulsion Laboratory, Pasadena, Calif., June 15, 1972.

2. Potter, P. D., "Network Engineering and Implementation: S- and X-Band Feed System," in *The Deep Space Network Progress Report*, Technical Report 32-1526, Vol. X, pp. 135–142, Jet Propulsion Laboratory, Pasadena, Calif., Aug. 15, 1972.

3. Woo, R. T., and Ludwig, A. C., "Low Loss Dichroic Plate," NASA Patent Application No. NPO 13171-1, Sep. 21, 1972.

4. Woo, R. T., "A Low-Loss Circularly Polarized Dichroic Plate," 1971 G-AP International Symposium, University of California, Los Angeles, Calif., Sep. 22–24, 1971.

5. Hannan, P. W., "The Element-Gain Paradox for a Phased-Array Antenna," *IEEE Transactions on Antennas and Propagation*, Vol. AP-12, No. 4, pp. 423–433, July 1964.

6. Chen, C. C., "Transmission of Microwave Through Perforated Flat Plates of Finite Thickness," *IEEE Transactions on Microwave Theory and Techniques*, Vol. MTT-21, No. 1, pp. 1–6, Jan. 1973.

7. Clauss, R. C., and Potter, P. D., "Improved RF Calibration Techniques – A Practical Technique for Accurate Determination of Microwave Surface Resistivity," in *The Deep Space Network Progress Report*, Technical Report 32-1526, Vol. XII, pp. 59–67, Jet Propulsion Laboratory, Pasadena, Calif., Dec. 15, 1972.

8. Ludwig, A. C., *Calculation of Scattered Patterns from Asymmetrical Reflectors*, Technical Report 32-1430, Jet Propulsion Laboratory, Pasadena, Calif., Feb. 15, 1970.

9. Potter, P. D., "S- and X-Band RF Feed System," in *The Deep Space Network Progress Report*, Technical Report 32-1526, Vol. VIII, pp. 53–60, Jet Propulsion Laboratory, Pasadena, Calif., Apr. 15, 1972.

10. Ho, W., et al., "Brightness Temperature of the Terrestrial Sky at 2.66 GHz," *J. Atmos. Sci.*, Vol. 29, Sep. 1972, pp. 1210–1212.

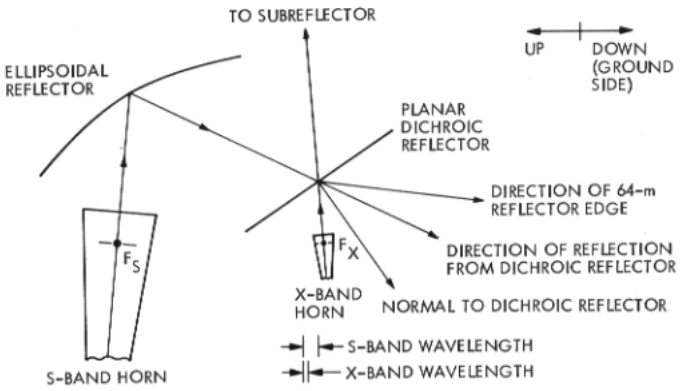

Fig. 1. Reflex feed system

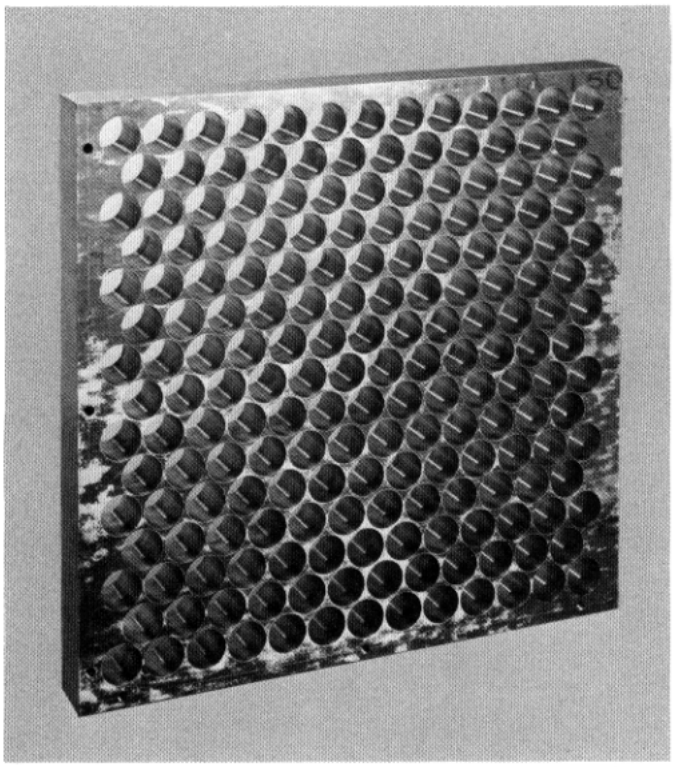

Fig. 2. Thick dichroic plate prototype

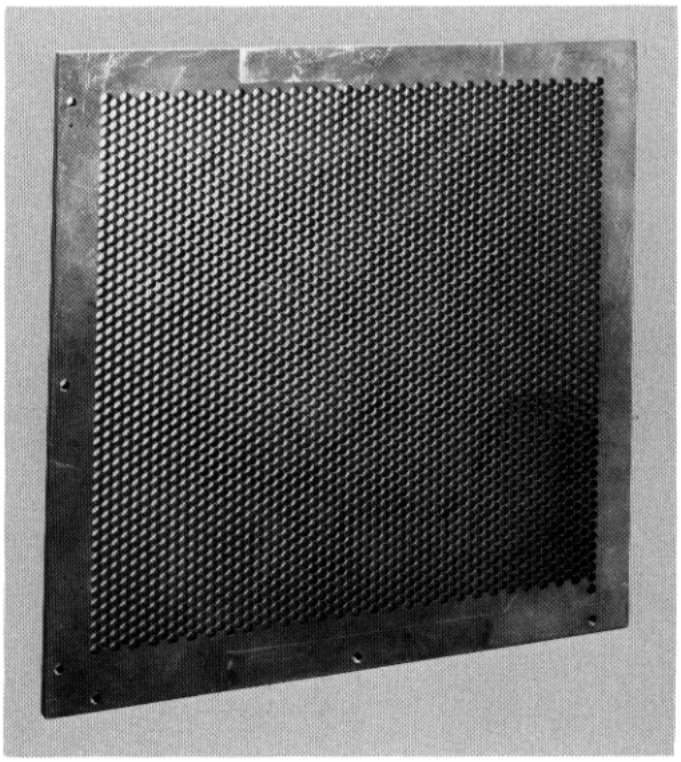

Fig. 3. Scale model of thick dichroic plate

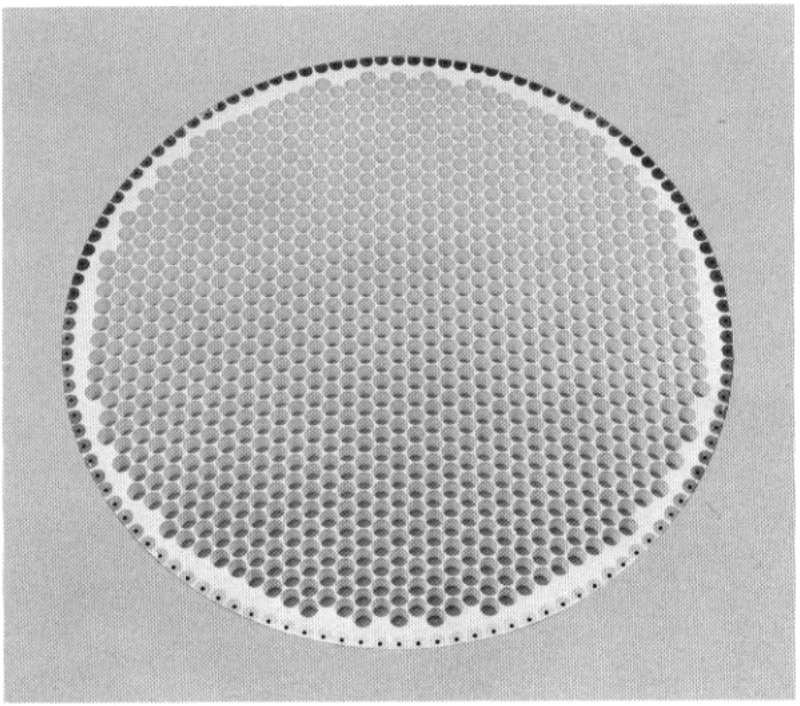

Fig. 4. DSS 14 dichroic reflector

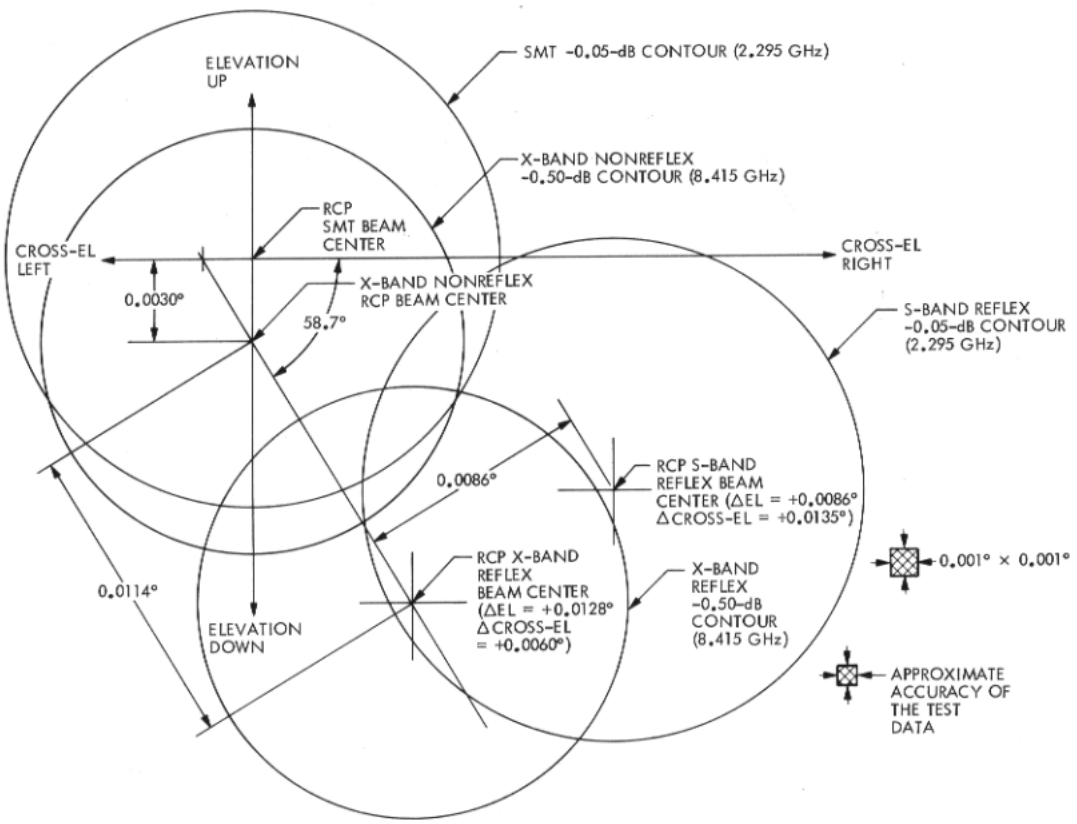

Fig. 5. DSS 14 SMT/MXK/reflex antenna beam positions, January 30, 1973

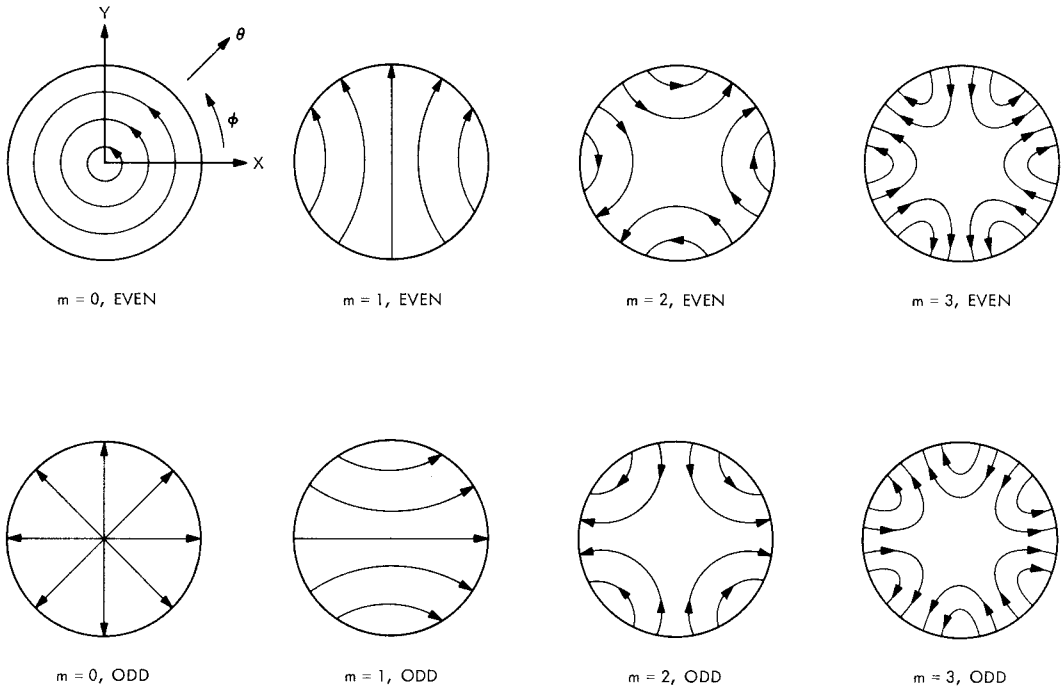

Fig. 6. Physical interpretation of m dependence

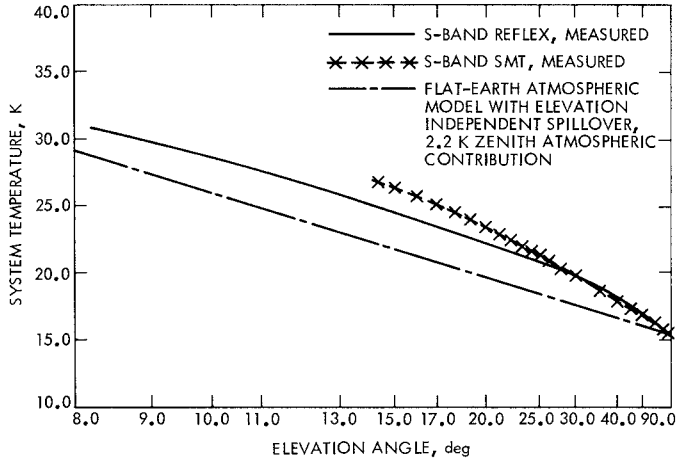

Fig. 7. DSS 14 S-band system noise temperature vs elevation angle, January 27–30, 1973

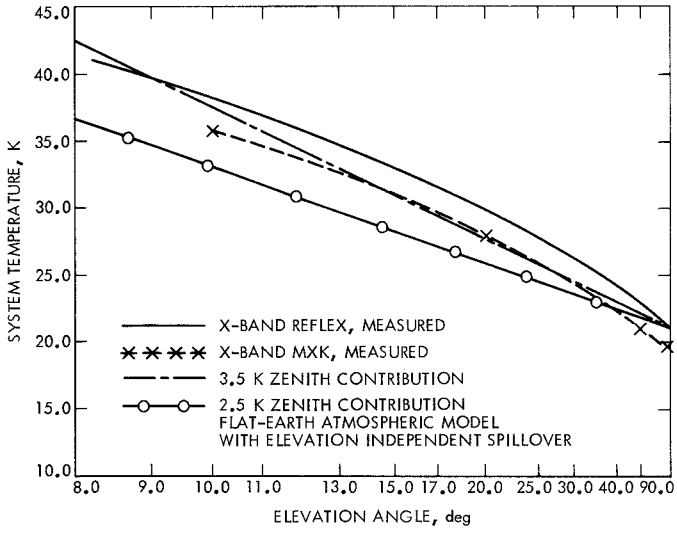

Fig. 8. DSS 14 X-band system noise temperature vs elevation angle, January 27–30, 1973